Electronic Supplementary Material (ESI) for ChemComm.

Identification and optical features of the $Pb_4Ln_2O_7$ series (Ln = La, Gd, Sm, Nd); genuine 2D-van der Waals oxides.

Marie Colmont,*[a] Kévin Lemoine,[a] Pascal Roussel,[a] Houria Kabbour,[a] Jacob Olchowk[b†] Natacha Henry,[b] Hans Hagemann,[b] and Olivier Mentré,[a]

a. Université Lille, CNRS, Centrale Lille, ENSCL, Université Artois, UMR 8181, Unité de Catalyse et Chimie du Solide, Lille, F-59000, France.

b. Dépt. de Chimie Physique, Université de Genève, 30, quai E. Ansermet, Geneva 4, CH-1211, Switzerland.

† Jacob Olchowka actual address is: CNRS, Université Bordeaux, Bordeaux INP, ICMCB UMR 5026, Pessac F-33600, France.

Supplementary Information

S1. Experimental Information

Synthesis.

Crystal growth: A mixture of PbO and La_2O_3 in ratio 6/2 was melted at 1000°C, cooled to 600°C with a rate of 3°C/h and then to room temperature at a rate of 15°C/h leading to orange-brown single crystals.

Powder synthesis: Polycrystalline powder samples were synthesized by conventional solid state reaction between $La(OH)_3$ PbO and Ln_2O_3 (Ln= Sm and Eu) in stoichiometric amount. After grinding precursors together, mixtures have been preheated at 600°C for 12h to remove volatile species. The reaction was complete after annealing at 900°C for 48h in an alumina crucible in air. Several intermediate grindings were necessary to obtain single crystalline-phases after checking XRD patterns. All final samples are bright brown.

Crystallographic studies.

A suitable crystal of $Pb_4La_2O_7$ with approximate dimension 0.13 × 0.09 × 0.005 mm^3 was selected under polarizing optical microscope and glued on a glass fiber for a single-crystal X-ray diffraction experiment. X-ray intensity data were collected on a Bruker -APEX2 CCD area-detector diffractometer using Mo-K_α radiation (λ = 0.71073 Å) generated with a 30W Incoatec micro-source. Several sets of narrow data frames were collected at different values of θ (3.01 to 26.29°), using 0.5° increments of ϕ or ω. Data reduction was accomplished using SAINT V8.27b. The substantial redundancy in data allowed a semi-empirical absorption correction (SADABS2012-1[1]) to be applied, on the basis of multiple measurements of equivalent reflections. The structure was solved by Charge Flipping algorithm using the SUPERFLIP software[2] and refined by full-matrix least-squares procedures using *CRYSTALS* program.[3] The bond valence sum calculations gives values close to the expected ones for all ions (see table S4).

Powder Diffraction Study.

X-ray powder diffraction analysis of the powder sample has been performed at room temperature in the angular range of 2θ 10–80° with a scan step width of 0.015° using a D8 Advance Bruker AXS diffractometer in Bragg Brentano geometry equipped with a 1D LynxEye detector.

High Temperature XRD study.

The temperature stability of the title compound was checked using HTXRD techniques on a Bruker D8 Advance diffractometer equipped with a high-temperature Anton Paar XRK900 chamber and a one dimensional X-ray detector (LynxEye) using Cu-Kα radiation under air. Data were collected over the range 10–50° in 2θ, with a 0.021° step and a time of 59 min per diagram from room temperature to 1175 K. Diffractograms were obtained every 50 K on heating.

Thermal Analysis.

Thermo gravimetric analysis (TGA) was performed using a Thermal Analysis instrument (TG92 Setaram) connected to a mass spectrometer (Omnistar), on 15 mg of sample. The weight loss was recorded under synthetic air, at a heating rate of 10 $K.min^{-1}$ from room temperature to 1273 K.

Infrared Spectroscopy.
Infrared spectra were measured between 4000 and 400 cm^{-1} with a Perkin–Elmer Spectrum Two TM spectrometer equipped with a diamond attenuated total reflectance (ATR) accessory.

Optical properties.
Photoluminescence excitation and emission spectra were collected on a Xenius Safas Monaco fluorescence spectrometer within the spectral range 250–800 nm at room temperature (290K). Each excitation spectrum was taken while observing emission at the predetermined emission wavelength maxima, and likewise, the emission spectra was taken while exciting at the sample's excitation wavelength maxima. The decay time measurements were performed at RT on a FluoroLog Horiba with a Xenon flash lamp as an excitation source.

UV/Vis spectra have been collected at room temperature with a Perkin Elmer Lambda 650 spectrophotometer in the 240–800 nm range using an integration sphere designed for the characterization of solids. The spectrum of the blank was measured before each sample measurement to calibrate the device.

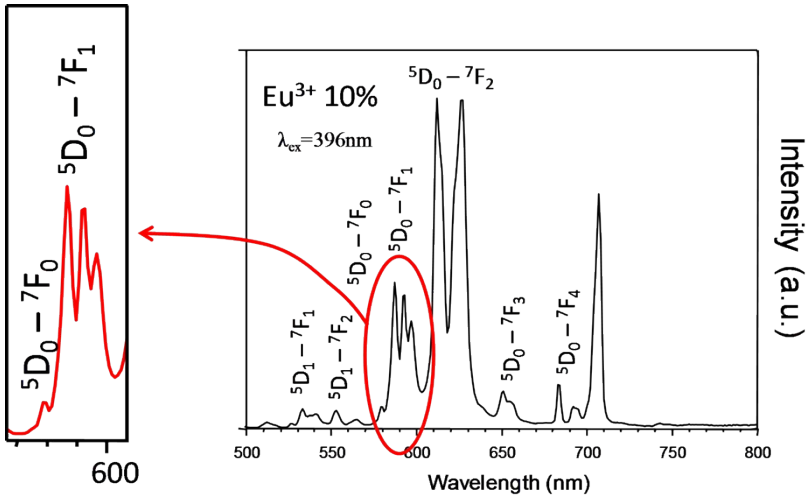

Figure S1. RT emission spectrum of $Pb_4La_2O_7 : Eu^{3+}$

Computational Methods.

Density functional theory (DFT) calculations were performed using the Vienna *ab initio* simulation package (VASP).[4] The calculations were carried out within the generalized gradient approximation (GGA) for the electron exchange and correlation corrections using the Perdew-Wang (PW91) functional and the frozen core projected wave vector method.[5,6] The full geometry optimizations were carried out using a plane wave energy cutoff of 550 eV and 10 *k* points in the irreducible Brillouin zone for all compounds. All structural optimizations converged with residual Hellman-Feynman forces on the atoms smaller than 0.03 eV/Å and led to reasonable structures regarding the distances and the local geometries (Table S5). The experimental structure matched well the optimized one, i.e. within a reasonable error expected for the GGA method. The relaxed structures were used for calculations of the electronic structure. For the later, we used a plane wave energy cutoff of 400 eV, an energy convergence criterion of 10^{-6} eV and 20 *k* points in the irreducible Brillouin zone.

S2. Crystal data and structural refinement parameters for $Pb_4La_2O_7$

Formula	**$Pb_4La_2O_7$**
Formula weight	1218.61
Temperature/K	293
Crystal color	orange
Crystal size/mm	0.126 × 0.095 × 0.005
Crystal system	triclinic
Space group	P-1
a/Å	7.7054(10)
b/Å	7.7262(10)
c/Å	10.1822(10)
α/°	72.574(10)
β/°	84.285(10)
γ°	61.737(10)
Volume/Å^3	508.77(12)
Z, $\rho_{calculated}$/g.cm^{-3}	2, 7.954
μ/mm^{-1}	74.15
Θ range/°	2.099 to 26.459
Limiting indices	$-9 \leq h \leq 9$, $-8 \leq k \leq 9$, $0 \leq l \leq 12$
Collected reflections	2046
Unique reflections	2038 [R_{int} =0.05]
Data/restraints/parameters	1707/0/84
Goodness-of-fit on F^2	0.953
Final R indices [I>2*σ*(I)]	R_1 = 0.0565 wR_2 = 0.0405
R indices (all data)	R_1 = 0.0518 wR_2 = 0.437
Largest diff. peak and hole/e.Å^{-3}	7.04/-4.45

S3. O(Pb,La)$_4$ oxo-centered tetrahedra and OPb$_3$ oxo-centered triangle in the crystal structure of $Pb_4La_2O_7$. The position of lone-pair is marked in grey.

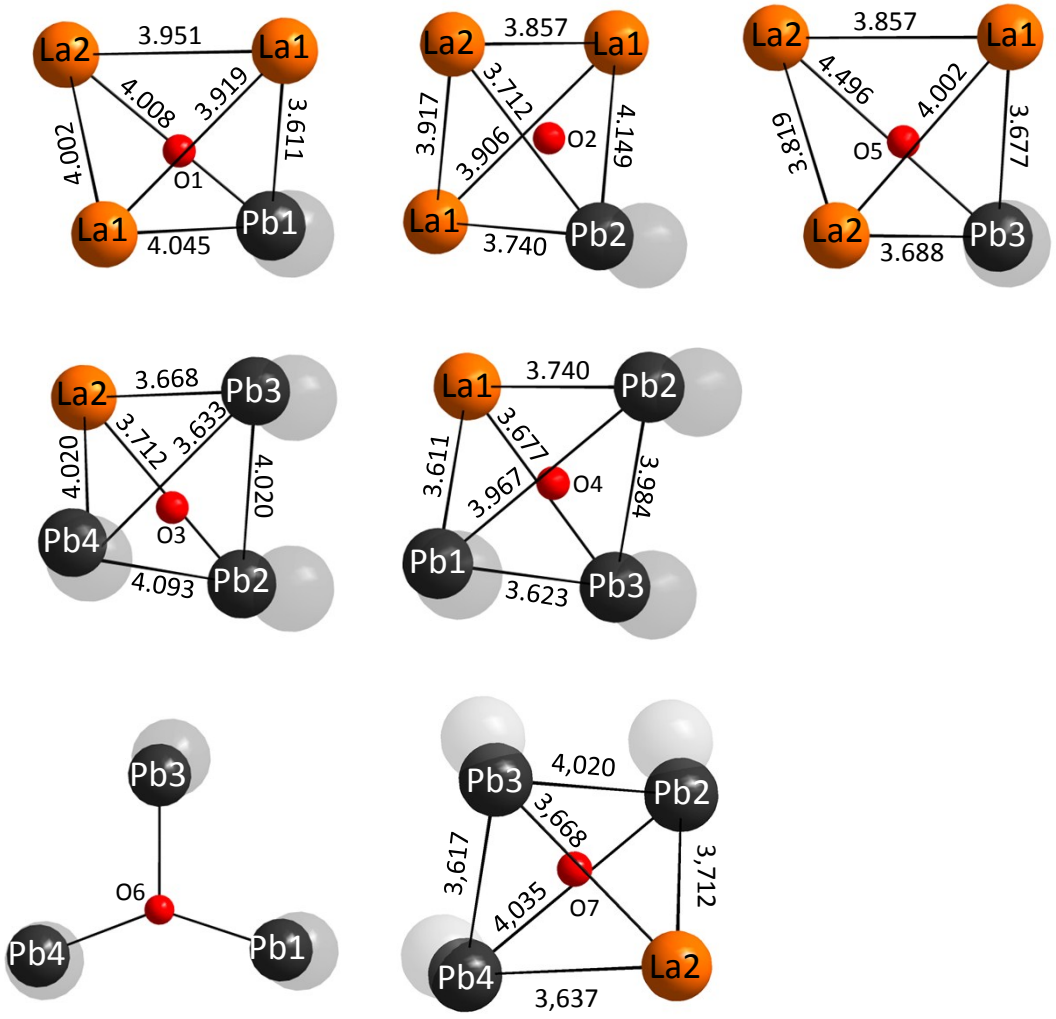

S4 . Atomic coordinates, calculated lone pair (LP) coordinates, bond-valence sums (B.V.S.) and displacement parameters (Å^2) for $Pb_4La_2O_7$.

Site	Partial charge	B.V.S.	X	Y	Z	Ueq	U11	U22	U33	U23	U13	U12
Pb1	+0.0691	1.90(3)	0.66399(8)	1.05583(9)	0.18652(6)	0.0132(2)	0.0108(3)	0.0128(3)	0.0170(3)	-0.0066(2)	0.0045(2)	-0.0051(2)
LP(1)			0.717555	0.079806	0.198656							
Pb2	+0.1457	1.86(3)	1.36596(9)	0.44614(9)	0.83582(6)	0.0125(2)	0.0108(3)	0.0126(3)	0.0141(3)	-0.0045(2)	0.0005(2)	-0.0053(2)
LP(2)			0.360810	0.4422611	0.841134							
Pb3	+0.1440	1.82(3)	0.82024(9)	0.90149(8)	0.84377(6)	0.0150(3)	0.0149(3)	0.0154(3)	0.0140(3)	-0.0058(3)	0.0009(2)	-0.0056(2)
LP(3)			0.797657	0.876129	0.842423							
Pb4	+0.0807	1.91(3)	0.85298(9)	0.43214(9)	0.81392(6)	0.0135(3)	0.0124(3)	0.0109(3)	0.0168(3)	-0.0058(3)	0.0027(2)	-0.0035(2)
LP(4)			0.827888	0.37223	0.790571							
La1	+2.1784	2.96(5)	0.50161(13)	0.76140(13)	0.46814(9)	0.0104(3)	0.0072(4)	0.0087(4)	0.0167(4)	-0.0044(3)	0.0028(3)	-0.0051(3)
La2	+2.0684	2.90(4)	1.00997(13)	0.73875(14)	0.53296(9)	0.0103(3)	0.0075(4)	0.0095(4)	0.0159(4)	-0.0044(3)	0.0021(3)	-0.0060(3)
O1	-0.8070	1.92(3)	0.6845(16)	0.9632(16)	0.4132(11)	0.013(2)						
O2	-0.8068	2.02(4)	1.3672(15)	0.5612(15)	0.6119(10)	0.0097(19)						
O3	-0.5164	1.94(3)	1.0477(17)	0.5734(17)	0.7929(12)	0.018(2)						
O4	-0.5219	1.93(3)	0.4665(16)	1.1514(17)	0.7919(11)	0.017(2)						
O5	-0.7859	1.78(3)	0.8543(16)	1.0439(16)	0.6258(11)	0.015(2)						

O6	-0.4502	1.86(3)	0.6465(19)	0.7458(19)	0.8096(13)	0.024(3)						
O7	-0.7981	1.91(3)	0.8330(16)	0.5261(17)	0.5886(11)	0.015(2)						

S5 . Main distances in triangular and tetrahedral OPb_3 and $O(Pb,La)_n$ units.

Central atom	neighbor	distance	Central atom	neighbor	distance	Central atom	neighbor	distance
O1 -	Pb1	2.198(10)	O2 -	La1	2.341(16)	O3 -	La2	2.551(9)
	La1	2.478(18)		La1	2.561(15)		Pb2	2.199(15)
	La1	2.523(13)		La2	2.510(14)		Pb3	2.485(13)
	La2	2.449(12)		Pb2	2.185(10)		Pb4	2.199(19)
O4 -	Pb1	2.212(19)	O5 -	La1	2.539(13)	O7 -	La1	2.496(12)
	La1	2.547(10)		La2	2.516(14)		La2	2.509(18)
	Pb2	2.205(15)		La2	2.497(15)		La2	2.464(14)
	Pb3	2.472(12)		Pb3	2.212(10)		Pb4	2.183(10)
O6 -	Pb1	2.151(12)						
	Pb3	2.281(19)						
	Pb4	2.170(13)						

S6. Reversible destruction under current atmosphere.

The as prepared sample has been let in a plastic box during two months. After checking it again using X-Ray diffraction, it evidenced a complete change with the presence of two different phases: $Pb_3(CO_3)_2(H_2O)_2$ [7] and $LaCO_3OH$.[8,9] The presence of water molecules as well as carbonates was confirmed by IR spectroscopy (figS6-1a). IR spectrum of the raw material was recorded. Four bands observed at 1400, 1059, 853 and 680cm^{-1} are strongly linked to the vibrational modes of the carbonate groups been respectively assigned to $\nu_3, \nu_1, \nu_2, \nu_4$. The peak around 3600$cm^{-1}$is assigned to the presence of water molecule (through O-H vibrations).[9]

The evolution of the sample was carefully checked. The just as synthesized powder sample was put in an alumina crucible inside a desiccator. A small beaker (10mL) of water was placed closed to it. The sample was analyzed by X-Ray diffraction every 12 hours. After 12 hours, additional peaks are observed closed to the tittle phase (fig S6-1b). They come from $Pb_3(CO_3)_2(H_2O)_2$. After 36 hours, other peaks related to $LaCO_3OH$ are observed. $Pb_4La_2O_7$ is still observed by in very small amount. It totally disappeared after 48 hours.

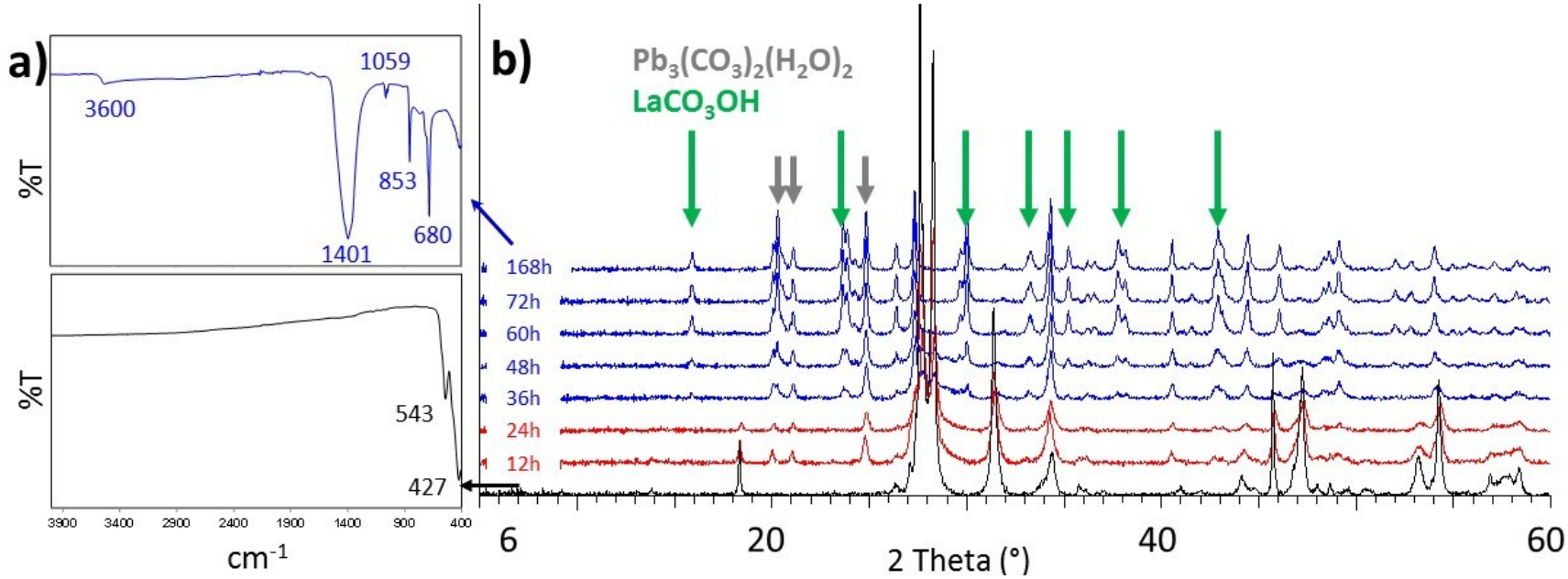

FigS6-1. IR spectra of $Pb_4La_2O_7$ a) just synthesized (in dark) and after two months (in blue), b) X-Ray diffraction evolution of raw $Pb_4La_2O_7$ after several hours.

After that, the modified sample was heated and followed in Situ using High Temperature X-Ray Diffraction (FigureS6-2). The sample was heated up to 900°C at a rate of 10°C/min and quickly cooled back to RT. The results show five different transitions:

1- at 245°C and leading to appearance of Pb_2OCO_3[10], $Pb_3(CO_3)_2(H_2O)_2$[7] and $LaCO_3OH$[11],

2- 330°C, water molecules and carbonates totally disappeared and oxides are synthesized in terms of α-PbO [12], PbO [13] and Pb_3O_4 [14],

3- 475°C, $La_{1.73}Pb_{2.27}O_{6.20}$ [15] appeared with α-PbO, PbO and Pb_3O_4,

4- 575°C Pb_3O_4 collapsed and finally,

5- 760°C the titled phase is obtained again as pure phase.

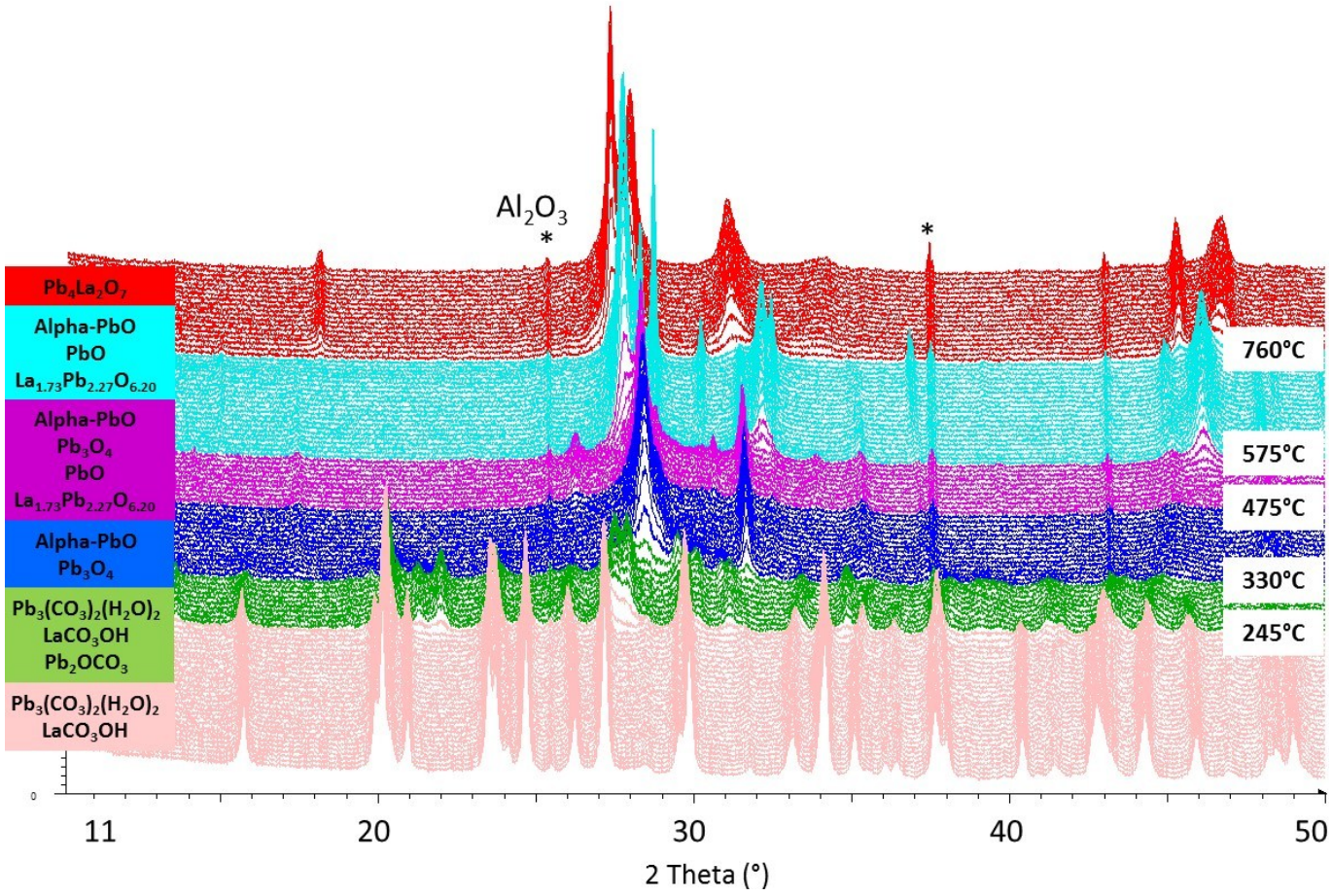

FigS6-2. HTXRD study of the modified sample. It shows five different phase transitions leading to the re-formation of $Pb_4La_2O_7$.

S7. DFT calculation

The total DOS (fig S7) shows basically two blocks in the valence band (VB): the lower VB in the range -7.7 to -5.2 eV and the upper part in the range -3.5 eV to the Fermi level (E_F).

In the upper VB, the *p* states of Pb are found with a small contribution of the Pb *s* states just below the Fermi level. O3 and O5 *p* states are found in the upper VB as well. Although they exhibit differences in the details of the DOS features due to their different environments ($O3La_3Pb$ and $O5LaPb_3$), they contribute rather similarly.

The conduction band (CB) is dominated by the 4*f* states of La in the range 4.5 to 5 eV. Lower in the CB, a smaller contribution in the range 2.3 to 3 eV is raising mostly from the Pb *p* states. The later constitute the bottom of the CB.

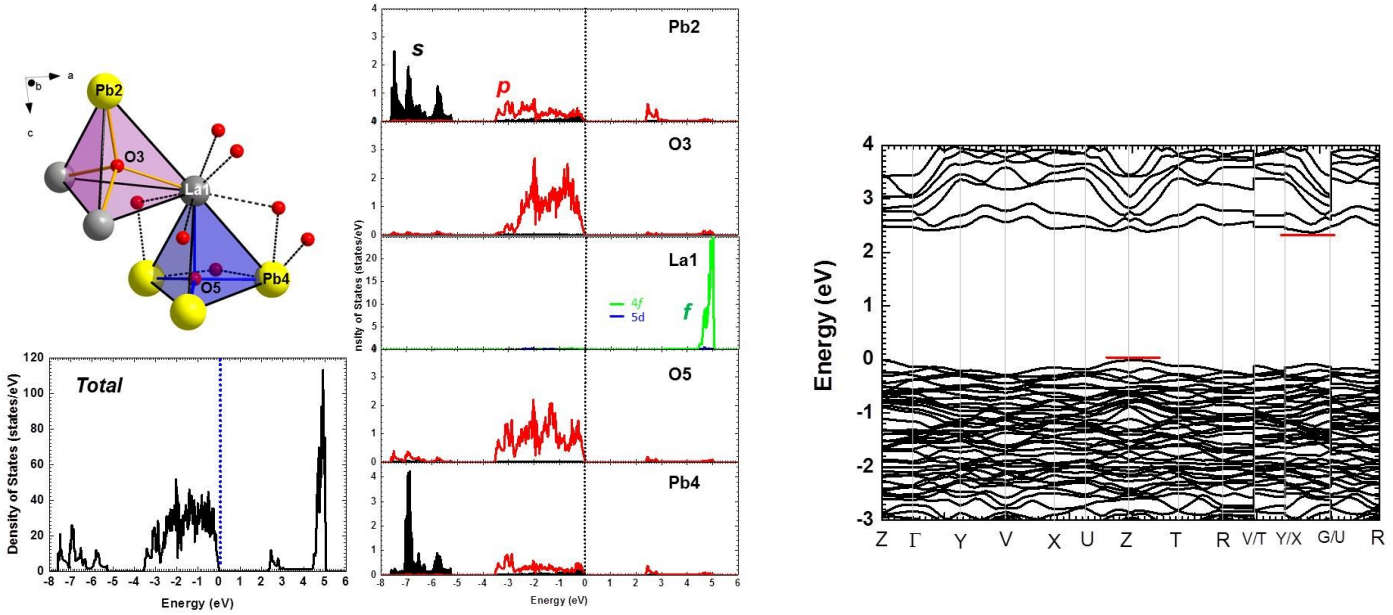

FigS7a. Total DOS of $Pb_4La_2O_7$ with contribution of each atom on the left and band structure on the right highlighting an indirect band gap.

The indirect band gap of the bulk turned into direct one when considering a monolayer modeled from the (a, b, 2c) supercell with a interleave distance of about 14 Å between the layers. This crossover is relatively common in true 2D-materials often related to electronic confinement, and has been detailed for instance in PbO.[16] However, the indirect nature of the crystalline phase is very subtle such that the change of band dispersion is minor.

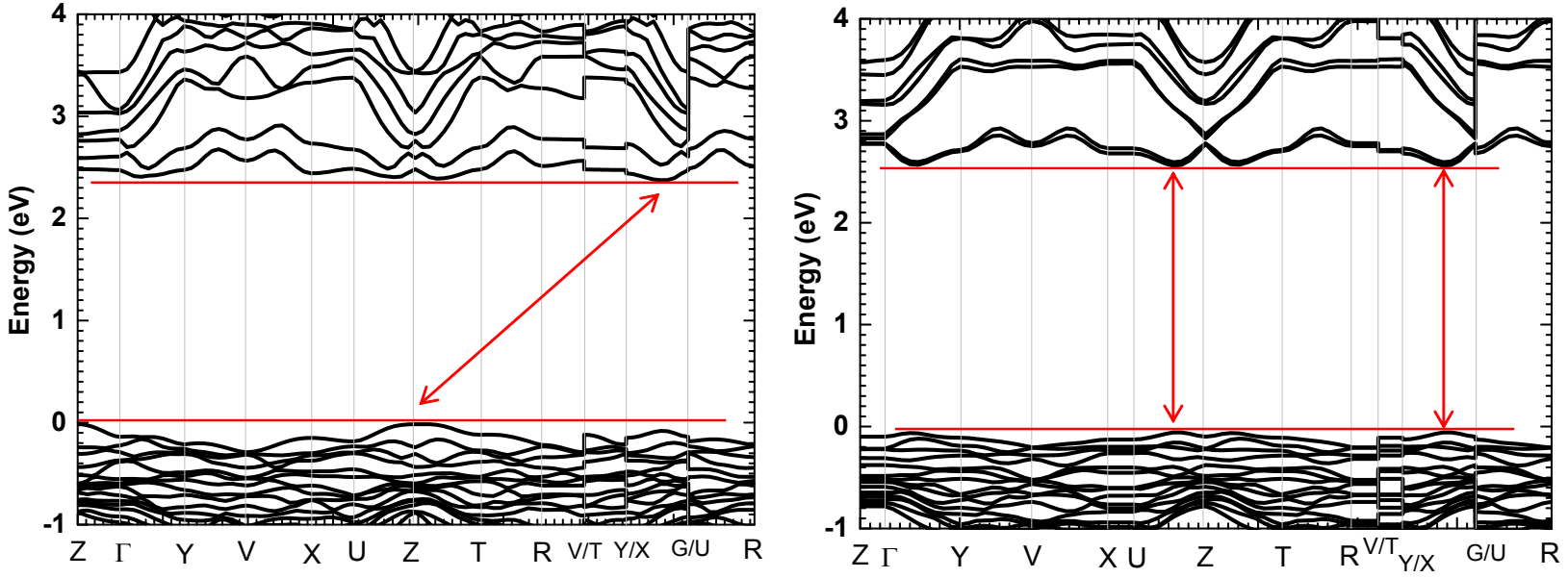

Fig.S7b: Band structures of the bulk compound (left) and of a monolayer modeled by a doubled cell along *c* with about 14 Å vacuum between each layer (one layer is removed in the supercell that contains two layers). Red lines are indicated to help pointing the CBM and the VBM. The arrows are indicating an indirect band gap for the bulk and direct band gap for the monolayer at several points of the IBZ.

In addition, the band structure represented on the right shows an indirect band gap with the maximum of the VB (located at Z) and the minimum of the CB (located between X and Γ) pointed in red on the figure.

S8. 2D behavior

The 2D behavior of the prepared sample was checked. First, after several grinding times varying from 5 to 45 minutes, the samples becomes amorphous, in good coherence with the separation of the flakes (Figure S8-a). Also preliminary tests of exfoliation were performed in butanol. Figure S8-b) show a positive Tyndall effect in agreement with the presence of nanoflakes. A TEM study performed on the exfoliated sample show particles of various thickness (related to the grey color of the particles) some of them being very bright so thin (Figure S8-c). The average size in shape is around 225nm as confirmed by DLS (Figure S8-d). The exfoliated flakes are neutral as shown Figure S8-e on the Potential Zeta analysis.

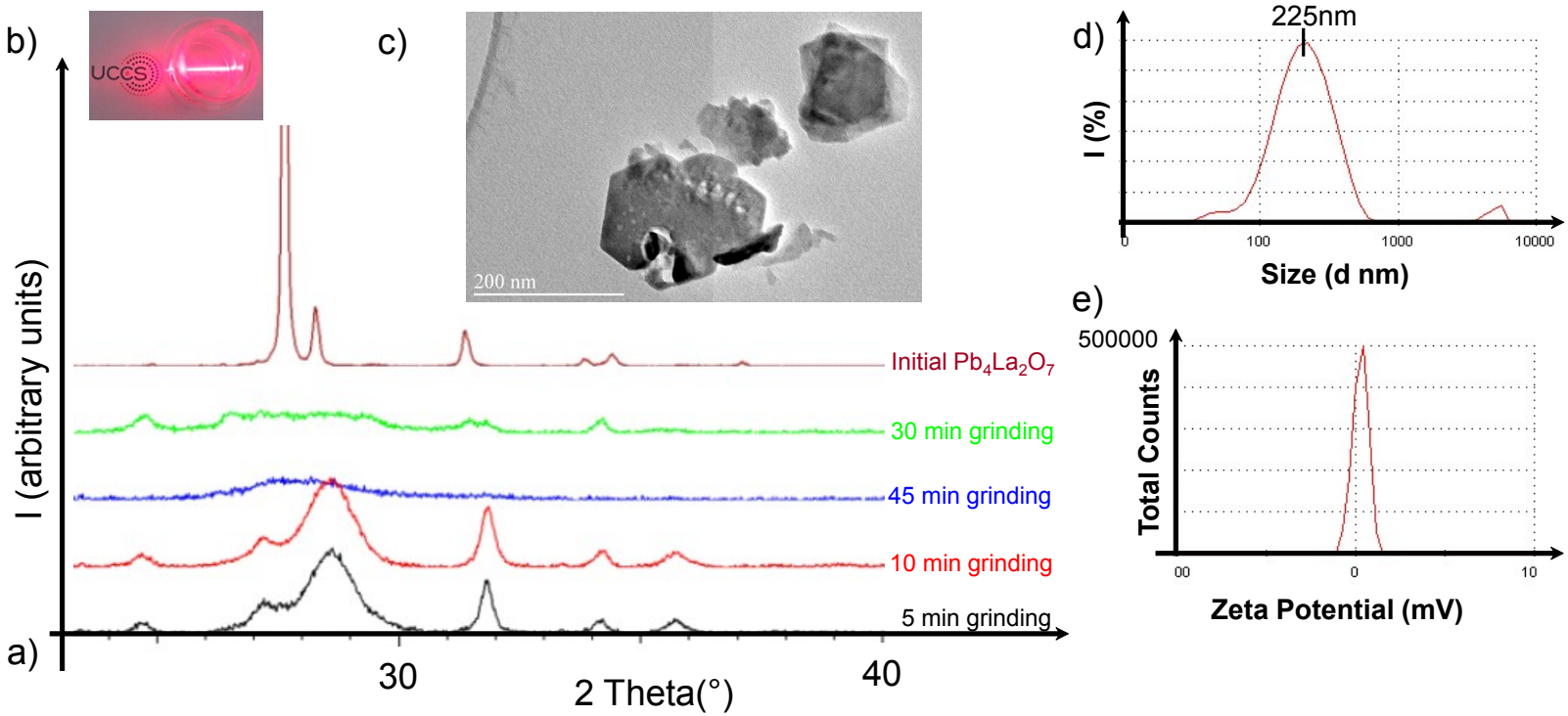

FigS8. a) XRDP performed after 5, 10, 30 and 45 minutes of grinding. Preliminary tests on exfoliation were performed in Butanol. b) Tyndall effect, c) TEM image, d) DLS and e) Zeta Potential analysis confirmed the presence of thin neutral nanoflakes.

REFERENCES

[1] G. M. Sheldrick, “SADABS, version2, University of Göttingen, Germany.” 2004.

[2] L. Palatinus and G. Chapuis, “SUPERFLIP – a computer program for the solution of crystal structures by charge flipping in arbitrary dimensions,” *J. Appl. Crystallogr.*, vol. 40, no. 4, pp. 786–790, Jul. 2007.

[3] P. W. Betteridge, J. R. Carruthers, R. I. Cooper, K. Prout, and D. J. Watkin, “*CRYSTALS* version 12: software for guided crystal structure analysis,” *J. Appl. Crystallogr.*, vol. 36, no. 6, pp. 1487–1487, Dec. 2003.

[4] Kresse, G. and J. Furthmüller, “Vienna Ab-initio Simulation Package (VASP).” 2012.

[5] G. Kresse, “From ultrasoft pseudopotentials to the projector augmented-wave method,” *Phys. Rev. B*, vol. 59, no. 3, pp. 1758–1775, Jan. 1999.

[6] J. P. Perdew and Y. Wang, “Accurate and simple analytic representation of the electron-gas correlation energy,” *Phys. Rev. B*, vol. 45, no. 23, pp. 13244–13249, Jun. 1992.

[7] P. Martinetto, M. Anne, E. Dooryhée, P. Walter, and G. Tsoucaris, “Synthetic hydrocerussite, 2PbCO(3) x Pb(OH)(2), by X-ray powder diffraction,” *Acta Crystallogr. C*, vol. 58, no. Pt 6, pp. i82–84, Jun. 2002.

[8] A. He *et al.*, “Preparation and Characterization of Lanthanum Carbonate Octahydrate for the Treatment of Hyperphosphatemia,” *J. Spectrosc.*, vol. 2013, pp. 1–6, 2013.

[9] R. Sarbajna, D. Sivalakshmi, K. Purandhar, and M. V. Suryanarayana, “Thermogravimetric Method Validation And Study Of Lanthanum Carbonate Octahydrate And Its Degradants,” pp. 2810–2820, Dec-2013.

[10] S. V. Krivovichev and P. C. Burns, “Crystal chemistry of basic lead carbonates. I. Crystal structure of synthetic shannonite, Pb2O(CO3),” *Mineral. Mag.*, vol. 64, no. 6, pp. 1063–1068, Dec. 2000.

[11] K. Michiba, T. Tahara, I. Nakai, R. Miyawaki, and S. Matsubara, “Crystal structure of hexagonal RE(CO3)OH,” *Z. Für Krist.*, vol. 226, no. 6, Jan. 2011.

[12] P. Boher, P. Garnier, J. R. Gavarri, and A. W. Hewat, “Monoxyde quadratique PbOα(I): Description de la transition structurale ferroe´lastique,” *J. Solid State Chem.*, vol. 57, no. 3, pp. 343–350, May 1985.

[13] P. Garnier, J. Moreau, and J. R. Gavarri, “Analyse de rietveld de la structure de Pb1−xTixO1+x par diffraction des neutrons,” *Mater. Res. Bull.*, vol. 25, no. 8, pp. 979–986, Aug. 1990.

[14] S. T. Cross, “The crystal structure of Pb3O4,” pp. 1107–1110, 1943.

[15] M. Troemel, *ICDD Grant-in-Aid*, Johann Wolfgang Goethe University, Frankfurt am Main, Germany, 1996.

[16] Y. Wang, Q. Zhang, Q. Shen, Y. Cheng, U. Schwingenschlögl, and W. Huang, “Lead monoxide: a two-dimensional ferromagnetic semiconductor induced by hole-doping,” *J. Mater. Chem. C*, vol. 5, no. 18, pp. 4520–4525, 2017.